

# Cold collision shift cancelation and inelastic scattering in a Yb optical lattice clock

A. D. Ludlow, N. D. Lemke, J. A. Sherman, and C. W. Oates  
*National Institute of Standards and Technology, 325 Broadway, Boulder, CO 80305, USA\**

G. Quéméner, J. von Stecher, and A. M. Rey  
*JILA, National Institute of Standards and Technology and University of Colorado, Boulder, CO 80309-0440*

Recently,  $p$ -wave cold collisions were shown to dominate the density-dependent shift of the clock transition frequency in a  $^{171}\text{Yb}$  optical lattice clock. Here we demonstrate that by operating such a system at the proper excitation fraction, the cold collision shift is canceled below the  $5 \times 10^{-18}$  fractional frequency level. We report inelastic two-body loss rates for  $^3P_0$ - $^3P_0$  and  $^1S_0$ - $^3P_0$  scattering. We also measure interaction shifts in an unpolarized atomic sample. Collision measurements for this spin-1/2  $^{171}\text{Yb}$  system are relevant for high performance optical clocks as well as strongly-interacting systems for quantum information and quantum simulation applications.

Large ensembles of ultracold atoms offer atomic clocks a measurement of the atomic state with high signal-to-noise ratio. For clocks utilizing optical transitions, this has the potential to yield time and frequency measurements with record levels of precision and speed (e.g. [1, 2]), directly benefiting the scientific and technological applications of these high performance clocks. However, large ensembles of cold atoms can lead to high number density and thus significant interatomic interactions. These interactions can perturb the clock transition frequency, compromising the accuracy and operation of the atomic standard. For example, in primary frequency standards based on an atomic fountain of laser-cooled cesium, cold collision shifts can become significant [3, 4] and can substantially influence the clock operation (e.g. [5–7]).

Optical lattice clocks, which probe large samples of laser-cooled atoms confined in an optical lattice potential, are also susceptible to cold collisions. Utilizing the ultra-narrow  $^1S_0$ - $^3P_0$  transition in two-valence-electron atoms, these systems are excellent candidates for realizing new levels of precision and accuracy in time and frequency measurement. However, non-negligible collision effects have been observed in lattice clocks using nuclear-spin-polarized, fermionic samples of  $^{87}\text{Sr}$  [8, 9] and  $^{171}\text{Yb}$  [10]. Measurement and control of these collisions therefore play a key role in the continued development of these standards. At the same time, the control of these interactions are an integral part of proposals for quantum information [11, 12] and quantum simulation of solid-state-analog Hamiltonians [13–15]. For  $^{87}\text{Sr}$ , the primary interaction giving the cold collision shift was identified as an  $s$ -wave interaction between atoms in non-identical superpositions of the clock states [9, 16, 17]. Under strong interactions, it was recently shown that the effect of  $s$ -wave interactions could be isolated, leading to a suppression of the cold collision frequency shift [16, 18].

In the case of  $^{171}\text{Yb}$ , however, it was shown that a  $p$ -wave interaction between atoms in the  $^1S_0$  and  $^3P_0$  electronic states was the dominant mechanism responsible

for the cold collision shift [19]. Unlike the  $s$ -wave case, such an interaction is less sensitive to small particle distinguishability between the ultracold fermions. Consequently, for atoms trapped in both 1-D and 2-D lattices (where, respectively, weak and strong interactions can occur) the observed shift exhibits roughly a linear dependence on the  $^3P_0$  excitation fraction (Fig. 1(a)). Moreover, in the weakly interacting regime of the 1-D lattice, it was seen that the cold collision shift crossed zero at a mean excitation fraction close to 0.5. In this work, we exploit this zero-crossing to demonstrate cancelation of the  $^{171}\text{Yb}$  cold collision shift in a 1-D optical lattice below the  $5 \times 10^{-18}$  fractional frequency level. The cancelation is enabled by the fact that near 50% excitation, the populations of the two electronic states of one atom induce equal collision shifts on the opposite states of another atom, leaving zero net shift for the clock transition [20]. The collision shift cancelation can thus be likened to the Stark shift cancelation which optical lattice clocks exploit by operating at the “magic” wavelength [21, 22]. Our uncertainty in this cancelation reaches below the smallest total uncertainty levels reported to date for any type of atomic clock, making it a powerful and pragmatic technique for mitigating the collisional shift in a lattice clock. In turn, control of the interactions at this level demonstrate the potential utility of such a system for quantum simulation and information applications. We also measure interactions relevant for achieving the shift cancelation, including the collision shift from an unpolarized sample of  $^{171}\text{Yb}$  and the two-body trap losses due to  $^3P_0$ - $^3P_0$  and  $^1S_0$ - $^3P_0$  inelastic scattering.

The  $^{171}\text{Yb}$  optical lattice clock is described in detail elsewhere [10, 19]. A thermal beam of Yb is cooled and loaded into a magneto-optical trap (MOT) operating on the  $^1S_0$ - $^1P_1$  transition, followed by a second, colder MOT utilizing the weaker  $^1S_0$ - $^3P_1$  transition. Atoms are then loaded into a 1-D optical lattice, which is formed with a focused standing wave using a laser at  $\lambda_{\text{magic}} \simeq 759$  nm. The atomic population is initially split between the two ground magnetic substates for this  $I = 1/2$  isotope, and

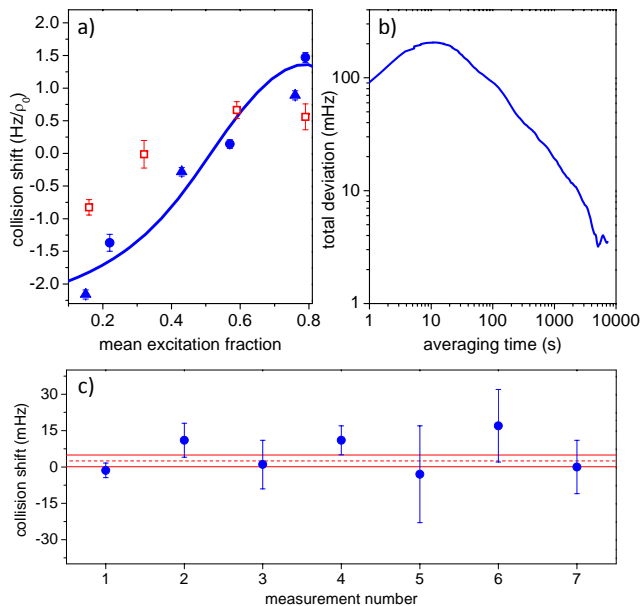


FIG. 1: (color online) (a) Cold collision shift as a function of mean excitation fraction. Measured for polarized  $^{171}\text{Yb}$  confined in a 1-D optical lattice, oriented vertically (filled triangles) or horizontally (filled circles). Open squares give the same measurement for an unpolarized atomic sample. (b) By operating at the proper excitation fraction, the cold collision shift is canceled. The measurement uncertainty for this cancellation is shown, given by the time-dependent total deviation (similar to two-sample Allan deviation [23]). (c) Measurement of the residual cold collision shift when operating at 51% excitation and an atomic density of  $\rho \simeq \rho_1$ . The red dashed line indicates the weighted mean of the seven measurements, +2.5 mHz, while the solid lines gives the one- $\sigma$  error bars of  $\pm 2.4$  mHz.

prior to spectroscopy the population is optically pumped to a single spin state. Depending on the trap depth of the lattice, the atoms have a temperature of  $5 - 10 \mu\text{K}$ , and we estimate the average atomic density can reach  $\rho_0 \approx 3 \times 10^{11}$  atoms/cm $^3$ . The atoms are then spectroscopically probed on the  $^1S_0$ - $^3P_0$  transition using Ramsey spectroscopy. The Ramsey pulse times used here are 5-10 ms, while the dark time is 80-150 ms. After multiple consecutive experimental cycles probing the clock transition, the cavity-stabilized probe laser is actively stabilized to the clock transition using an acousto-optic modulator. The cold collision shift is determined from the measured frequency difference between interleaved atomic samples of high and low density.

Measurement of the collision shift in a 1-D lattice is shown as filled points in Fig. 1(a), as a function of excitation fraction (during the Ramsey dark time). The theoretical calculation of the shift using a  $p$ -wave model is also shown (solid line). In the model, the dominant interaction,  $V_{eg}$ , is between  $^1S_0$  and  $^3P_0$  atoms, and a weaker interaction between two excited state atoms,  $V_{ee} = 0.1 \times V_{eg}$ , is also included [19]. The shift has a

zero value near 50% excitation, and this zero-crossing is the focus of our attention here. In order to determine the precise excitation corresponding to zero shift, we first stabilized the  $\pi$ -polarized component of the probe laser intensity, monitoring the optical power (with a polarization analyzer) after the vacuum chamber of the atom system. Second, we implemented a scheme for real-time measurement of the excitation fraction interspersed between cycles of usual Ramsey spectroscopy. These excitation-only measurements were accomplished by simply turning off the second Ramsey pulse and measuring the ground and excited atomic populations after the dark time. We then slightly adjusted the stabilized probe power to keep the measured excitation fraction constant during each shift measurement.

The precision to which we could measure the zero-crossing is given by the clock instability during interleaved measurements of high and low atomic density. Here, our measurement stability benefits from recent improvements to the cavity-stabilized laser used to probe the clock transition [1]. Fig. 1(b) shows the precision of one such measurement, where we observed a collision shift of -1.4 (3) mHz after 14500 s of averaging. Fig. 1(c) shows the result of seven similar measurements, taken sequentially over the course of several weeks and with different measurement durations. For all but one measurement, the mean excitation fraction was controlled to  $51 \pm 0.3 \pm 1.3 \%$ , where the first uncertainty term corresponds to fluctuations in the realized excitation fraction and the second corresponds to the systematic uncertainty for determining the absolute excitation value. (For data point number two, the excitation fraction was set to 1% higher; we thus applied a  $-5$  mHz correction to the measured collision shift, as determined from the slope of the curve in Fig. 1(a).) The weighted mean of the seven measurements (red lines) is 2.5 (2.4) mHz (reduced  $\chi^2 = 1.04$ ). This corresponds to a fractional shift of  $4.8$  ( $4.6$ )  $\times 10^{-18}$  of the transition frequency, and demonstrates the smallest measurement of a collision shift in a lattice clock.

In order to routinely implement this collision shift cancellation in the Yb optical lattice clock, we consider the robustness of this technique to relevant experimental conditions. For an operational density of  $\rho_1 \simeq 3 \times 10^{10}$  atoms/cm $^3$ , a change in 1% of the excitation fraction leads to a change in collision shift of  $\sim 1 \times 10^{-17}$ . As described above, it is straightforward to keep the excitation fixed at or below the 1% level. However, a complication arises due to a time-varying excitation fraction during the Ramsey dark time as a consequence of lattice trap loss. Particularly, we have observed inelastic two-body losses involving both  $^3P_0$ - $^3P_0$  and  $^1S_0$ - $^3P_0$  interactions. With both  $^1S_0$  ( $g$ ) and  $^3P_0$  ( $e$ ) populations present, the

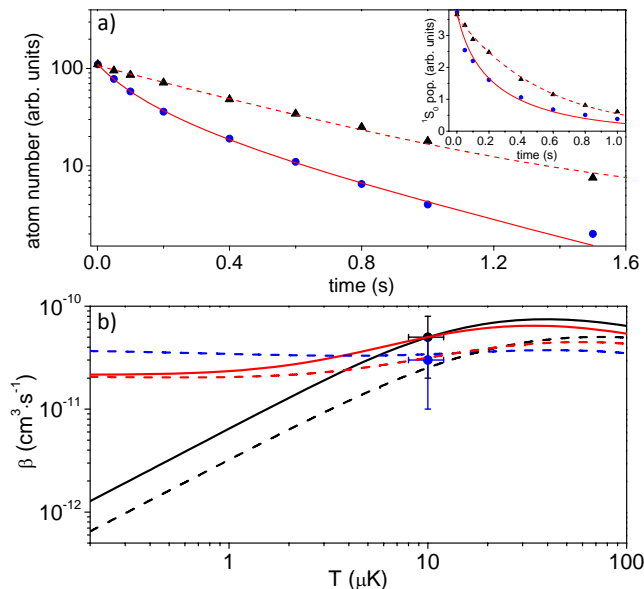


FIG. 2: (color online) (a) Yb atom number loss. Black triangles indicate trap loss of  $^1S_0$  atoms, with the dashed curve an exponential fit. The blue circles give trap loss of  $^3P_0$  atoms, with the solid curve a one- and two-body loss fit. The inset shows  $^1S_0$  atom number loss for the case of a pure  $^1S_0$  sample (black triangles) and a mixed sample of  $^1S_0$  and  $^3P_0$  atoms (blue circles). The former is fit with a simple exponential, while the latter curve includes  $^3P_0$ - $^3P_0$  and  $^1S_0$ - $^3P_0$  two body losses. (b) Two body loss rates,  $\beta$ , as a function of temperature. Circles are experimental measurements. Dashed curves are calculated with full loss probability ( $p_{\text{ls}} = 1$ ) and solid curves are for  $p_{\text{ls}} = 0.8$  and  $\delta = 0.51\pi$ . Black is for a nuclear-spin-polarized sample of  $^3P_0$  atoms ( $\beta_{ee}$ ), red for an unpolarized sample of  $^3P_0$  atoms ( $[\beta_{ee} + \tilde{\beta}_{ee}]/2$ ), and blue is for  $^1S_0$ - $^3P_0$  interactions ( $\beta_{eg}$ ).

number density rate equations are:

$$\begin{aligned}\dot{n}_g(t) &= -\Gamma_g n_g(t) - \beta_{eg} n_g(t) n_e(t) \\ \dot{n}_e(t) &= -\beta_{ee} n_e(t)^2 - \Gamma_e n_e(t) - \beta_{eg} n_g(t) n_e(t)\end{aligned}$$

In the case of a single population ( $n_g$  or  $n_e$ )  $\beta_{eg}$  loss can be ignored. Fig. 2(a) shows  $^1S_0$  trap loss (black triangles, for a pure sample of  $^1S_0$  atoms), with a one body loss fit yielding a trap lifetime of  $1/\Gamma_g = 480$  (20) ms. Also shown is  $^3P_0$  trap loss (blue circles, for a pure sample of  $^3P_0$  atoms). This population experiences notably stronger decay at high densities, and good fit requires both one-body ( $\Gamma_e$ ) and two-body ( $\beta_{ee}$ ) losses. After integrating the losses over the spatial extent of a single lattice site, as well as across the distribution of occupied sites, we find  $1/\Gamma_e = 520$  (28) ms and  $\beta_{ee} = 5 \times 10^{-11} \text{ cm}^3/\text{s}$ , somewhat larger than the  $^3P_0$ - $^3P_0$  decay measured in  $^{88}\text{Sr}$  [24, 25]. Because the absolute atomic density is difficult to calibrate, the uncertainty in  $\beta_{ee}$  is estimated as 60%.

The inelastic two-body loss for  $^3P_0$  atoms can be considered with a single atom-atom channel, time-

independent quantum formalism similar to [26, 27]. Lacking an accurate  $\text{Yb}_2$  potential in the literature, the short range physics is described here by a boundary condition at an interatomic separation  $R_0 = 20 a_0$  ( $a_0$  is the Bohr radius), represented by two parameters: (i) an accumulated phase shift,  $0 \leq \delta \leq \pi$ , due to the unknown short-range potential from  $R = 0$  to  $R = R_0$ , and (ii) a loss probability,  $0 \leq p_{\text{ls}} \leq 1$  at  $R = R_0$  ( $p_{\text{ls}} = 1$  represents full loss probability,  $p_{\text{ls}} = 0$  is lossless). The long range physics is accurately described by a van der Waals interaction, with  $C_6 = 3886$  a.u. given by [28]. The Schrödinger equation is numerically solved from  $R_0$  to  $R \rightarrow \infty$ , and the cross section is computed as a function of the collision energy. The thermalized rate coefficients are found by averaging the cross sections with a Maxwell-Boltzmann distribution of collision energies for a given temperature.

For the case of full loss probability,  $\beta_{ee}$  is computed as a function of temperature, and is shown in Fig. 2(b) (black dashed curve). Here, the rates are universal and do not depend on the other parameter  $\delta$  [26, 27]. The interaction involves two identical fermions, and thus quantum statistics dictates that the interactions must be odd partial waves, notably  $p$ -wave at these ultracold temperatures. As two excited atoms approach each other, those which successfully tunnel through the  $p$ -wave barrier are assumed to inelastically scatter with unit probability ( $p_{\text{ls}} = 1$ ). This assumption seems reasonable due to the large number of exit collision channels available to a pair of atoms with high internal energy. For an unpolarized sample of  $^3P_0$  atoms (here with equal  $m_I = \pm 1/2$  populations), interactions between distinguishable atoms also include an  $s$ -wave term, and the loss rate for distinguishable  $^3P_0$  atoms is labeled  $\tilde{\beta}_{ee}$ . The total loss rate for the unpolarized sample, given by the average of  $\beta_{ee}$  and  $\tilde{\beta}_{ee}$ , is shown in Fig. 2(b) as a red dashed curve ( $p_{\text{ls}} = 1$ ). Experimentally, we observed identical loss rates within 10% for a polarized and an unpolarized sample at  $10 \mu\text{K}$ , given by the black circle in Fig. 2(b). Since the full loss model predicts unequal loss rates for polarized and unpolarized samples at  $10 \mu\text{K}$ ,  $^3P_0$  atoms may not be lost with full unit probability at short range. Instead, using short range parameters of  $p_{\text{ls}} = 0.8$  and  $\delta = 0.51\pi$  for both polarized and unpolarized case, shown respectively as black and red solid lines in Fig. 2(b), we found better agreement with the experimental data, suggesting a deviation from the universal regime with full loss.

For a mixed population of  $^1S_0$  and  $^3P_0$  atoms, we observed additional loss through  $\beta_{eg}$ . Fig. 2(a) inset highlights this by comparing  $^1S_0$  trap loss for two different atomic samples: with (blue circles) and without (black triangles) the presence of  $^3P_0$  atoms. The additional loss is particularly notable at short times where both  $^1S_0$  and  $^3P_0$  populations are large. The additional loss is consistent with a  $^1S_0$ - $^3P_0$  two-body loss rate at the level of  $\beta_{eg} = 3 \times 10^{-11} \text{ cm}^3/\text{s}$ . Using the same formalism as

above for  $p_{\text{ls}} = 1$ , and a value of  $C_6 = 2709$  a.u. [28] for these distinguishable atoms,  $\beta_{eg}$  is computed and shown as the blue dashed curve in Fig. 2(b). The good agreement with our experimental measurement at  $10 \mu\text{K}$  suggests that  $^1S_0 + ^3P_0$  collisions are universal with a full loss probability at short range. This is noteworthy because for molecular states correlating to a  $^1S_0$  and  $^3P_0$  atom pair, only the  $^1\Sigma_g^+$  ground state (correlating to the  $^1S_0$ - $^1S_0$  state) lies at lower energy, and long-range coupling to this state is spin-forbidden.

In general, all of these loss processes lead to a time-dependent excitation fraction during the Ramsey dark time. This, in turn, affects the balance between  $^1S_0$  and  $^3P_0$  collisionally induced energy shifts. For simplicity, we can easily operate at a lower atom number density, reducing not only the collisionally-induced shifts, but also the two-body inelastic losses. At the same time, the number of quantum absorbers remains well in excess of 1000, in order to accommodate a high signal-to-noise ratio. At a density of  $\rho_1$ , the excitation fraction over a dark time of  $T = 150$  ms changes by only several percent. We therefore take the time-averaged value to indicate the excitation fraction where the shift is canceled.

Any degree of imperfect polarization of the nuclear spin state introduces a host of other possible atomic interactions. In  $p$ -wave, the  $V_{eg}^-$  interaction, which shifts the singlet state  $(|eg\rangle - |ge\rangle)/\sqrt{2}$ , becomes allowed. Furthermore, the distinguishability between different nuclear spin states allows  $s$ -wave interactions  $U_{gg}$ ,  $U_{ee}$ , and  $U_{eg}^+$ . In  $^{171}\text{Yb}$ , both the  $s$ - and  $p$ -wave  $|gg\rangle$  interaction terms are small [29]. However, the remaining interactions can alter the observed collision shift from the spin-polarized case. For this reason, high polarization purity is important for optical lattice clocks. Here, we benefit from the simple structure in  $^{171}\text{Yb}$ , which has  $I = 1/2$ . The population, which starts as an equal mixture of the two spin states  $m_I = \pm 1/2$  is readily optically pumped to a single spin ground state with 99% purity. The optical pumping utilizes the  $^1S_0$  ( $I = 1/2$ ) -  $^3P_1$  ( $I = 3/2$ ) transition with  $\sigma$ -polarized light, in the presence of a bias magnetic field (5 G). The polarization purity is directly measured by observing the absence of a clock excitation spectrum for the unpopulated spin state. This polarization purity could be further enhanced by using the clock transition to resonantly excite a single spin state, and then heating away the remaining ground state population.

To quantify the effect of imperfect polarization, we measure the collision shift as a function of excitation for unpolarized atoms (equal mixture of both spin states) as shown with open squares in Fig. 1(a). Since, during spectroscopy, a weak bias field (1 G) lifts the degeneracy of the  $\pi$ -transitions from the two spin states, here the excitation fraction is defined as that for the particular spin state being resonantly excited, not accounting for the other ‘spectator’ spin state. In general, the measured shifts are smaller than for the spin-polarized case, imply-

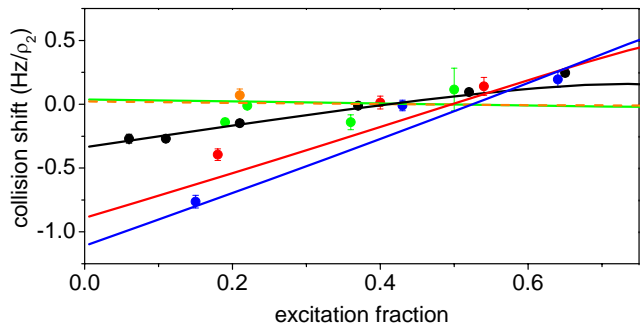


FIG. 3: (color online) Cold collision shift as a function of excitation for a polarized sample in a 2-D lattice, for different Ramsey times.  $\rho_2$  is a typical 2-D lattice density, where 25% of the atoms are doubly occupied in a lattice site with density of  $4 \times 10^{12}$  atoms/cm<sup>3</sup>. Circles correspond to experimental measurements, and solid curves are theoretical calculations [19]. In both cases, blue is a Ramsey time of  $T = 10$  ms, red is 40 ms, black is 80 ms, green is 160 ms, and orange is 210 ms.

ing that competing interactions have the opposite sign as those in the polarized case. Notably, the measured zero-crossing in the shift occurs at a lower excitation fraction (around 40%), leaving a net positive shift at 51%, where the shift is zero for the spin polarized case. Based upon these measurements, we determine a 1% polarization impurity will not affect the shift zero-crossing at or above the level measured in Fig. 1(c).

We have shown that the cold collision shift can be canceled at the  $5 \times 10^{-18}$  level in a 1-D optical lattice clock of  $^{171}\text{Yb}$ . Other implementations may be suitable for reducing the clock shift at or below this level. For example, in a 2-D optical lattice clock, strong interactions can lead to a decay of the collision shift [19, 30]. In particular, longer Ramsey dark times lead to smaller shifts and can reduce the shift dependence on excitation fraction (slope of curves in Fig. 3), making it attractive for shift reduction or cancellation. Care must be taken since, as we have observed both experimentally and theoretically, the interactions can also reduce Ramsey fringe contrast (experimentally this effect is notably strong for long Ramsey times in a 2-D lattice). Alternatively, the 2-D lattice system also exhibits a zero crossing in the shift versus excitation. However, strong interactions can move the zero-crossing excitation with a nonlinear dependence on interaction strength (Fig. 3), and thus the weak interactions of the 1-D lattice may be easier to control.

The 3-D optical lattice continues to be an interesting choice [21], where it is straightforward to achieve high atom number with an average of  $\ll 1$  atom per lattice site. The small fraction of lattice sites with double occupancy will exhibit very strong interactions, which may be further exploited to reduce the shift from these atoms. Doubly-occupied sites could also be eliminated using photoassociation losses [31] or more directly via the two-body

losses observed here. Furthermore, the 3-D optical lattice system may exhibit kinematic suppression of the atomic interactions which yield the shifts [32]. Indeed, these rich atomic systems will undoubtedly continue to offer many interesting phenomena in 1-, 2-, and 3-D confinement.

The authors gratefully acknowledge assistance from Y. Jiang, and financial support from NIST, NSF-PFC, AFOSR, and ARO with funding from the DARPA-OLE.

---

\* Electronic address: ludlow@boulder.nist.gov

- [1] Y. Y. Jiang, A. D. Ludlow, N. D. Lemke, R. W. Fox, J. A. Sherman, L. S. Ma, and C. W. Oates, *Nature Photonics* **5**, 158 (2011).
- [2] M. Takamoto, T. Takano, and H. Katori, *Nature Photonics* **5**, 288 (2011).
- [3] K. Gibble and S. Chu, *Phys. Rev. Lett.* **70**, 1771 (1993).
- [4] P. Leo, P. Julienne, F. Mies, and C. Williams, *Phys. Rev. Lett.* **86**, 3743 (2001).
- [5] F. P. Dos Santos, H. Marion, S. Bize, Y. Sortais, A. Clairon, and C. Salomon, *Phys. Rev. Lett.* **89**, 233004 (2002).
- [6] T. Heavner, S. Jefferts, E. Donley, J. Shirley, and T. Parker, *Metrologia* **42**, 411 (2005).
- [7] K. Szymaniec, W. Chalupczak, E. Tiesinga, C. J. Williams, S. Weyers, and R. Wynands, *Phys. Rev. Lett.* **98**, 153002 (2007).
- [8] A. D. Ludlow, T. Zelevinsky, G. K. Campbell, S. Blatt, M. M. Boyd, M. H. G. de Miranda, M. J. Martin, J. W. Thomsen, S. M. Foreman, J. Ye, et al., *Science* **319**, 1805 (2008).
- [9] G. K. Campbell, M. M. Boyd, J. W. Thomsen, M. J. Martin, S. Blatt, M. D. Swallows, T. L. Nicholson, T. Fortier, C. W. Oates, S. A. Diddams, et al., *Science* **324**, 360 (2009).
- [10] N. D. Lemke, A. D. Ludlow, Z. W. Barber, T. M. Fortier, S. A. Diddams, Y. Jiang, S. R. Jefferts, T. P. Heavner, T. E. Parker, and C. W. Oates, *Phys. Rev. Lett.* **103**, 063001 (2009).
- [11] D. Hayes, P. S. Julienne, and I. H. Deutsch, *Phys. Rev. Lett.* **98**, 070501 (2007).
- [12] A. V. Gorshkov, A. M. Rey, A. J. Daley, M. M. Boyd, J. Ye, P. Zoller, and M. D. Lukin, *Phys. Rev. Lett.* **102**, 110503 (2009).
- [13] A. V. Gorshkov, M. Hermele, V. Gurarie, C. Xu, P. S. Julienne, J. Ye, P. Zoller, E. Demler, M. D. Lukin, and A. M. Rey, *Nat. Phys.* **6**, 289 (2010), ISSN 1745-2473.
- [14] M. A. Cazalilla, A. F. Ho, and M. Ueda, *New Journal of Physics* **11**, 103033 (2009).
- [15] M. Foss-Feig, M. Hermele, V. Gurarie, and A. M. Rey, *Phys. Rev. A* **82**, 053624 (2010).
- [16] A. M. Rey, A. V. Gorshkov, and C. Rubbo, *Phys. Rev. Lett.* **103**, 260402 (2009).
- [17] K. Gibble, *Phys. Rev. Lett.* **103**, 113202 (2009).
- [18] M. D. Swallows, M. Bishof, Y. Lin, S. Blatt, M. J. Martin, A. M. Rey, and J. Ye, *Science* **331**, 1043 (2011).
- [19] N. D. Lemke, J. von Stecher, J. A. Sherman, A. M. Rey, C. W. Oates, and A. D. Ludlow, arXiv:1105.2014.
- [20] Shift cancellation occurs near 50% mean excitation for even large atomic sample inhomogeneity; however in the limit of small inhomogeneity, a given atom experiences the same shift in each atomic state and thus a shift cancellation on the transition.
- [21] H. Katori, M. Takamoto, V. G. Palchikov, and V. D. Ovsiannikov, *Phys. Rev. Lett.* **91**, 173005 (2003).
- [22] J. Ye, H. J. Kimble, and H. Katori, *Science* **320**, 1734 (2008).
- [23] C. A. Greenhall, D. A. Howe, and D. B. Percival, *IEEE Transactions on Ultrasonics Ferroelectrics and Frequency Control* **46**, 1183 (1999).
- [24] A. Traverso, R. Chakraborty, Y. N. M. de Escobar, P. G. Mickelson, S. B. Nagel, M. Yan, and T. C. Killian, *Phys. Rev. A* **79**, 060702 (2009).
- [25] C. Lisdat, J. S. R. V. Winfred, T. Middelmann, F. Riehle, and U. Sterr, *Phys. Rev. Lett.* **103**, 090801 (2009).
- [26] Z. Idziaszek and P. S. Julienne, *Phys. Rev. Lett.* **104**, 113202 (2010).
- [27] Z. Idziaszek, G. Quemener, J. L. Bohn, and P. S. Julienne, *Phys. Rev. A* **82**, 020703(R) (2010).
- [28] V. A. Dzuba and A. Derevianko, *J. Phys. B: At. Mol. Opt. Phys.* **43**, 074011 (2010).
- [29] M. Kitagawa, K. Enomoto, K. Kasa, Y. Takahashi, R. Ciurylo, P. Naidon, and P. S. Julienne, *Phys. Rev. A* **77**, 012719 (2008).
- [30] K. Gibble, 2010 IEEE International Frequency Control Symposium pp. 56–58 (2010).
- [31] T. Akatsuka, M. Takamoto, and H. Katori, *Phys. Rev. A* **81**, 023402 (2010).
- [32] K. Gunter, T. Stoferle, H. Moritz, M. Kohl, and T. Esslinger, *Phys. Rev. Lett.* **95**, 230401 (2005).